Submitted to Review of Scientific Instruments

UCRL-19756
Preprint

A MAGNETIC MONOPOLE DETECTOR UTILIZING SUPERCONDUCTING ELEMENTS

Luis W. Alvarez, Maurilio Antuna, Jr., Roscoe A. Byrns, Philippe H. Eberhard, Robert E. Gilmer, Egon H. Hoyer, Ronald R. Ross, Hans H. Stellrecht, John D. Taylor, and Robert D. Watt

April 1970

AEC Contract No. W-7405-eng-48

LAWRENCE RADIATION LABORATORY
UNIVERSITY of CALIFORNIA BERKELEY

A MAGNETIC MONOPOLE DETECTOR UTILIZING SUPERCONDUCTING ELEMENTS*

Luis W. Alvarez, Maurilio Antuna, Jr., Roscoe A. Byrns, Philippe H. Eberhard, Robert E. Gilmer, Egon H. Hoyer, Ronald R. Ross, Hans H. Stellrecht, John D. Taylor, and Robert D. Watt†

Lawrence Radiation Laboratory
University of California
Berkeley, California 94720

April 1970

Abstract

An electromagnetic detector has been built to extend the search for magnetic monopoles to the lunar sample returned during the Apollo missions. It is sensitive to the minimum magnetic charge allowed by Dirac's theory, and permits analysis of a sample without changing any of its properties.

The apparatus consists of a superconducting niobium sensing coil with a core at room temperature, shorted by a superconducting mechanical switch and protected against the effects of variable ambient magnetic field by an adjacent shield made of superconducting lead. Characteristic features, performance, and sample containers are described.

Introduction

This is the description of a detector for magnetic monopoles which utilizes only the electromagnetic properties of those particles and does not rely on their ionizing properties. Monopoles are particles that would interact with a magnetic field just as electric charges interact with an electric field. That is, they would act as a source for the magnetic field and would be accelerated by it. They would be stable and have a magnetic charge g given by

$$g = \nu g_0, \tag{1}$$

where, according to Dirac's theory,[1] ν is an integer and g_0 is the minimum value for a magnetic charge. In the Gaussian system of units,

$$g_0 = \frac{e}{2}\frac{hc}{e^2} = \frac{e}{2}\frac{1}{\alpha}. \tag{2}$$

Since $1/\alpha \approx 137$, this equation says that the value of the smallest magnetic charge (measured in cgs emu) is about 68.5 times the electron charge (measured in cgs esu).

The existence of magnetic monopoles would give credence to the only known explanation for the extraordinarily precise phenomenon of electric charge quantization.[2] According to a recent theory,[3] the most fundamental particle, the building block of the universe, would have both a magnetic and an electric charge.

Searches at high energy accelerators have not produced monopoles by bombarding matter with protons of energies as high as 70 GeV,[4] even though these experiments should have produced them if production cross sections were as low as 2×10^{-41} cm^2. The only source of protons with appreciably higher energies is the primary cosmic radiation, with its power-law spectrum extending up 10^{11} GeV. Other experiments[5-6]

searching large quantities of matter have not discovered a single monopole even though it was reasonable to assume that monopoles produced by the primary cosmic rays would have ended up by being trapped there. The advantage of the lunar sample over these materials stems from its great age (the time it has been exposed to cosmic radiation) and from the fact that monopoles would have been trapped there immediately after they had been created by collision of a cosmic ray proton with a nucleon of the lunar surface and had slowed down. No assumption concerning their migration in the atmosphere is required to assess the fate of the monopoles on the lunar surface.

A second source of monopoles could be a monopole component of the cosmic radiation. Such monopoles could be created by collisions of high energy cosmic ray particles with interstellar gas, or could have been created in the "big bang" or in other energetic astrophysical events. Monopoles from any of these sources would also have been slowed down and trapped by the lunar material.

Therefore, a proposal to search for monopoles in the Apollo lunar sample was submitted to NASA in 1966.[7] Acceptance was subject to several constraints on the handling of the precious lunar sample. In particular, NASA specified that the material

(a) remain in vacuum,

(b) remain at normal temperature,

(c) maintain its physical integrity (no cutting or melting of the rocks),

(d) be limited in acceleration to prevent damage, and

(e) never be exposed to magnetic fields much greater than the earth's field.

Moreover, any detector used had to be sensitive to a fraction of the charge g_0 to insure that noise would be no problem of any importance even when detecting a monopole of minimum charge. Reliability was imperative because of the schedule imposed by operating in the Lunar Receiving Laboratory.[8]

Detection Principle

In our equipment the presence of a monopole would be detected by the magnetic charge that it would confer to the whole sample. There would be a flux emitted by the sample equal to

$$\Phi = 4\pi g = n\Phi_0, \tag{3}$$

where $\Phi_0 = 4 \times 10^{-7}$ gauss-cm^2 and n is the integer of Eq. (1).

If such a sample were passed through a coil (Fig. 1), it would induce an electromotive force associated with the change of flux in the coil's circuit.[9] If the coil is part of a closed superconducting circuit carrying a current I, the net effect will be a change of I.[10]

$$\Delta I = N n \Phi_0 / L, \tag{4}$$

where ΔI = change in current I,

N = number of passes of the sample,

n = number of turns in the coil,

L = self inductance of the coil.

A known current is introduced in the circuit, the sample is circulated N times, and then the current is measured. From the current change ΔI the sample magnetic charge can be determined. Appendix I contains a description of the interaction between a monopole and a superconducting loop.

In our equipment, a superconducting switch is connected in parallel with a superconducting sensing coil (Fig. 2). When the sample is being run the switch is closed, hence the coil is shorted so that circuit is the loop of Fig. 1. The current is measured from the voltage pulse generated across the coil by opening the switch. The pulse is transferred outside the cryostat, amplified, and finally recorded on an oscilloscope.

Cryogenic Equipment

The detector has three independent circuits, each consisting of a sensing coil, a switch, and a set of shielded cables leading out of the cryostat. For the operation, only one circuit is necessary. The other circuits are provided for reliability.

Each sensing coil is made of 1200 turns of 0.020-in. niobium wire and has a self-inductance of 78 mH. To induce a small reference flux in the sensing coil, an auxiliary coil fed by a current supply is provided (Fig. 2). It has four turns of copper wire and a mutual inductance of 204 μH with each sensing coil.

The superconducting switch, shown in Fig. 3, has a movable cone that can be brought in contact with both terminals of the switch at the same time. Superconductivity is provided by coating all parts with 60 Pb-40 Sn solder. The movable cone is attached by means of a rod to a pneumatic cylinder operated at room temperature. Contact pressure and closing and opening speeds are varied by regulating gas pressures. The switch is operated remotely by a solenoid valve which controls the gas flow to the cylinder. Its response is sharp, with resistance going from zero to infinity in less than 100 μsec. A detailed description of the switch and its operation is given in Appendix II.

The cryostat is shown in Fig. 4. The superconducting elements are immersed in liquid helium. The liquid helium container and liquid nitrogen heat shields are placed inside a vacuum chamber. The vacuum chamber is traversed by a tube of 3-3/8 in. i.d. where sample containers are transported at room temperature and pressure through the sensing coils. This tube and the corresponding coaxial tube in the liquid helium container are made of fiberglass-epoxy laminate to limit eddy currents when the switch is being opened. One hundred thirty layers of 0.00025-in. aluminized Mylar between the tubes are used to reduce heat loss. Total cryostat thermal loss is 4.2 watts (6 liters of liquid helium per hour).

To guard against false signals induced by any change in the ambient magnetic field, it is necessary to apply an effective magnetic shield. This shield, shown on Figs. 2 and 4, consists of a superconducting sheet of lead surrounding the coil area and extending as a small cylinder for 4 diameters on both sides from away from the coil. It reduces the effect of external field changes in any direction by more than a factor of 10^6, while it affects the signal expected due to passage of a monopole by about 20% from the value predicted by Eq. 4. (See Appendix I.) Because of the size of the shielding inside the helium container, overall dimensions of the cryostat are 8 ft long (in the direction of coil axis), 4 ft wide, and 7 ft tall. Further description will be found in Appendix III.

Amplifier

The voltage pulse generated when the switch is opened has a time integral proportional to the self-inductance of the sensing coil and the current I in the loop. The response of the amplifier of Fig. 2 to such a voltage pulse has a shape like each of the three signals of Fig. 5.

The difference in height between the maximum and the minimum, the "peak-to-peak amplitude" of the signal, is proportional to the time integral of the input pulse, and is rather insensitive to small variations in its shape. In addition the signal amplitude remains measurable for wide variation in triggering level of the scope.

The amplifier output shape is produced by the circuit of Fig. 4. The circuit consists of an operational amplifier, a differentiating RC circuit as the input impedance, an integrating RC circuit of the same time constant to close the feedback loop, and an additional integrator with the same time constant on the output. To maximize the signal to noise ratio the time constant is set as short as possible consistent with variation in switch-opening times. Parameters of the amplifier were varied in order to optimize the time constant and the input impedance. In addition, the input capacitor prevents thermoelectric effects from generating uncontrolled currents in the sensing circuit. Best performance was obtained by using an additional feature not shown on Fig. 4, a 1:6 transformer before the amplifier and a capacitor in series with the primary. (Circuit diagrams are given in Appendix V, Figs. 19 and 20.)

The detector sensitivity is measured by placing a long calibrated solenoid through the detecting coil with the ends protuding well beyond the shielding. Turning on a current in the solenoid simulates the passage of a known magnetic charge along a path represented by the solenoid. (See Appendix I.) The relation between magnetic charge and signal on the scope is therefore established for a single pass. Table I lists quantitative changes in variables which all evoke the same system response.

Sample Container and Transport System

The sample container, shown in Fig. 7, is designed to maintain the sample in a 4-mm-i.d. tube. The container diameter is maximized consistent with the size of the tube that traverses the cryostat in order to process as much material as possible. The design, seal details, and performance are given in Appendix IV. The sample transport system is shown in Fig. 4. A three-wheeled (rubber-tired) cart connected to a 0.014-in. Mylar belt carries the sample container around the loop. The belt is driven by a crowned rubber-faced 18-in.-diameter pulley set, coupled to a variable-speed electric motor. Speeds of about 10 ft/sec are available, but the NASA-imposed lunar sample acceleration limit of 1g reduced the operating velocity to 5 ft/sec, corresponding to a period of about 4 sec for 1 revolution.

The lead shield assembly were designed to isolate the sensing coil as much as possible from vibrations that might result in a displacement of the coil with respect to the lead shield. This would cause flux variations and hence current changes in the sensing coil because of the time-dependent field trapped by the lead. To further minimize this effect, a system of coils around the cryostat reduced the magnetic field in the sensing region to a few milligauss while the assembly was cooled to liquid helium temperature and the lead became superconducting.

Operation

After cooldown, the sensing circuit is checked for superconductivity, i.e., its ability to conserve the current for a long time. Its resistance has to be less than 10^{-9} Ω and consistent with zero, and the switch, when opened, should produce signals of proper shape and height before the

circuit is considered satisfactory. Then, sample analysis proceeds.

A sample is loaded into the container, which is then attached to the transport system. The electronics is then tested by use of the auxiliary coil and the current supply shown in Fig. 2. With the superconducting switch open, a current of 20 μA is fed through the auxiliary coil. When the current supply is turned off, a signal is recorded on the oscilloscope. It is called the "reference signal" (Number 1 on Fig. 5). It represents a change of flux equivalent to circulating a monopole of charge $1000\,g_0$ one time or of charge g_0 a number of times $N_0 = 1000$. Its amplitude should be of standard size. Then a test of the switch, coil, and vibration effects is performed by turning the current on again, closing the superconducting switch, and then turning the current supply off so that a standard current is stored in the superconducting loop. The sample is circulated a few times and stopped outside the shielding. The switch is opened and the resulting signal stored on the scope. This signal we call the "short store" signal (Number 2 on Fig. 5). It should also be of the standard size. Finally, we repeat the operations used in getting the short-store signal but this time circulating the sample a large number of times, $N = 400$. This is the "measurement signal" (Number 3 on Fig. 5).

The magnetic charge g of the sample is determined from the difference between the amplitude V of the measurement signal and the standard amplitude V_0 determined from an average of many reference signals,

$$g = \frac{V - V_0}{V_0} \frac{N_0}{N} g_0 . \qquad (5)$$

Since a zero magnetic charge produces a standard signal, the proper operation of the equipment is tested even when samples without monopoles are run. A change in signal size indicates the presence of a monopole or a malfunction of the equipment. When this happens, the equipment is checked and the sample rerun. The presence of a monopole would be revealed by reproducible measurement signals V different from V_0, identical at each run, when the equipment is found to be functioning properly. The signals of Fig. 5 indicate no magnetic charge in a sample.

Performance

When a sample is passed through the detector N times, the measurement error σ_g of the magnetic charge is

$$\sigma_g = (\sigma/N)\, g_0, \tag{6}$$

where σ is the 1-standard-deviation uncertainty of the measurement signals, expressed in terms of the number of passes of the charge g_0 that would produce the same deviation.

The reference signals have a 1-standard-deviation spread equivalent to 25 passes. This can be explained by the noise of the operational amplifier. Referring to Table I, we see this is equivalent to a field change of 6×10^{-5} Gauss, or a current change of 1.4 nA in the sensing coil. The energy associated with 1.4 nA in a 78-mH coil is about 0.5 eV. The 1-standard-deviation spread of both the short-store and measurement signals is equivalent to 45 passes. The increase in spread of these signals over the reference signals is attributed to additional noise due to switch opening and inherent variations in the mechanical position of the detecting coil. Since this noise figure is the same for both short-

store and measurement signals, it shows that the uncertainty in the measurement of the magnetic charge is indeed inversely proportional to the number of passes N, as in Eq. (6). For N = 400 and σ = 45, as in the operation with the lunar sample, the uncertainty of the measurement is 0.11 g_0, from Eq. (6).

Figure 8 shows the equipment installed in the Lunar Receiving Laboratory. Twenty-eight samples of lunar material of a total weight of 8.4 kg were examined there during August 1969. The magnetic charge of all samples was measured and found to be consistent with zero and inconsistent with g_0 or any larger charge. From this experiment upper limits for the production cross section and flux of monopoles in cosmic rays were inferred.[11]

ACKNOWLEDGMENTS

For help with the design, construction, and test operation, we are indebted to G. Eckman, L. Foley, H. Hagopian, I. Laker, W. Lawton, J. Remenarich, R. Rinta, M. Saarloos, and S. Yee. We gratefully acknowledge the help we have received from the staff of the Lunar Receiving Laboratory.

APPENDIXES

I. Interaction Between a Monopole and a Superconducting Loop

Maxwell Equations with Magnetic Charges

If magnetic charges exist, additional terms should be introduced into Maxwell's equations. To take into account the magnetic charge density ρ_m as a source for the magnetic field $\vec{B}$, using the cgsm system, we write

$$\operatorname{div} \vec{B} = 4\pi \rho_m . \qquad (I.1)$$

Moving magnetic charges are represented by a magnetic current density $\vec{j}_m$. To respect Lorentz invariance, $\vec{j}_m$ has to interact with the electric field $\vec{E}$ according to

$$\operatorname{curl} \vec{E} + \partial \vec{B}/\partial t = -4\pi \vec{j}_m . \qquad (I.2)$$

Equation (I.2) shows that a moving monopole generates an electric field around its path in a way similar to the way an electric charge generates a magnetic field (see Fig. 9). If the monopole travels in a coil, such electric field generates an electromotive force $\mathcal{E}$ in the coil equal to the integral of $\vec{E}$ along the wire,

$$\mathcal{E} = n\, 4\pi g \frac{dN}{dt} = \frac{dF}{dt} , \qquad (I.3)$$

where n = the number of turns of the coil,

$\frac{dN}{dt}$ = the number of monopoles of charge g passing per unit of time,

F = the flux of vector $\vec{B}$ in the coil.

Superconducting Loop

If the coil is part of a superconducting loop, as in Fig. 1, the electromotive force $\mathcal{E}$ must be zero. Integrating Eq. (I. 3) over time with $\mathcal{E} = 0$, we get

$$\Delta F = n N 4\pi g, \qquad \text{(I. 4)}$$

where ΔF = variation of the flux F,

N = number of passes made in the time interval considered.

In the simple diagram of Fig. 1, the change of F can be due only to the change in current I, when the monopole has returned to the same position after N revolutions:

$$L \Delta I = Nn 4\pi g, \qquad \text{(I. 5)}$$

where L = self-inductance of the coil.

Equation (I. 5) is equivalent to Eq. (4) when Eq. (3) is taken into account.

In the absence of magnetic charge, Eqs. (I. 1) and (I. 2) belong to the Maxwell equations, but with ρ_m and $\vec{J}_m = 0$; (I. 4) expresses the well-known law of flux conservation in a superconducting loop. We call $4\pi \rho_m$ and $4\pi \vec{J}_m$ the "missing terms" of Maxwell's equations. Equation (I. 4) shows that the flux change ΔF can be measured correctly and if the circuit stays superconducting, there is no possible background in this mode of detection for monopoles.

Shielding and Calibration

Because of magnetic fields generated by the environment, F is expressed by

$$F = LI + F', \qquad \text{(I. 6)}$$

where F' is the flux induced in the circuit by external causes.

To be able to measure ΔF from ΔI, the induced flux F' must be controlled. That is the reason for the lead shield shown on Fig. 2. It protects the circuit against variation of the ambient field. However, that shield is also a superconducting loop surrounding the path of the sample. A magnetic charge contained in a sample would induce a flux in the shielding and, by induction, there would be a contribution to F' from the currents in the shield.

After the switch shown in Fig. 2 has been opened, the flux in the coil is not the same as before sample circulation, but is changed by the ratio $\Delta F'_{m}$, the flux induced by the current in the shielding generated by the magnetic charge. Therefore, the flux variation ΔF_m measured when opening the switch is

$$\Delta F_m = \Delta F - \Delta F' \quad (I.7)$$

Both ΔF and $\Delta F'$ are proportional to the magnetic charge g, and to N, therefore

$$\Delta F'_m = K_n N 4\pi g = K \Delta F, \quad (I.8)$$

where K_n is a reduction factor.

We have measured K and found it to be 0.83 by using a long solenoid carrying a known flux through the detector, along the path of the sample. Equation (I.2) shows that the same effect can be produced by $\frac{\partial B}{\partial t}$ and by j_m. Therefore a change in the flux of B in a small area simulates exactly a flux of magnetic charge through the same area. Turning on the solenoid has the same effect as carrying a monopole from the location of one pole of the solenoid to the location of the other. Of course the solenoid poles were protruding well outside the shielding on either

side, so their exact location did not have any appreciable effect on the induced flux F.

II. Superconducting Switch Requirements

The superconducting switch of Fig. 2 permits accurate current measurements by the method previously described. It must not generate currents or voltages in the system when the switch is closed.

If no current variation is to result from a long running time without magnetic charge, switch resistance must be very low. A resistance of $10^{-7}\Omega$ would cause a 1% signal variation over 2 hours. Superconductivity was required for the switch to avoid possible thermoelectric effects and resistance effects.

Since some samples to be run in the detector have magnetic moments, the switch must be capable of carrying the currents induced in the coil when a magnetized sample is being tested without turning normal (i.e., resistive). For a sample with a moment of 200 emu, currents as high as 10 mA would be generated. At opening, the constants of the amplifier which provide the best signal-to-noise ratio require that the voltage integral be developed across the coil over a fraction of a millisecond. In this period of time the switch is transformed from a superconducting to a very highly resistant connection. Under typical operating conditions, signal distortion would occur if the switch were still partially conducting 100 μsec after it first showed resistance.

The design of the cryostat is such that partial disassembly is required in order to gain access suitable for working on switches with hand tools. When they are in the cryostat this disassembly would require

a minimum of 100 hours lost operating time if it became necessary to work in the switch area when the cryostat is at cryogenic temperatures. Therefore, the switch should be capable of reliable operation over reasonably long periods without maintenance. Even so, it is highly desirable to be able to remove the switch from the cryostat without extensive disassembly.

Another consideration in the design of the switch is the helium-consumption rate. Heat leak from cryogenic to ambient regions should be small. Also, transfer losses should be kept to a minimum by reducing the fill frequency. As switch height increases, the reservoir space above the switch is reduced. If the switch is to be completely covered by liquid helium, each additional inch of switch height reduces the time between transfers by 30 min.

Design

A switch that meets these requirements is shown in Fig. 3. Figure 4 is a photograph of a switch of this design which has been used in the detector. In making a switch the contact points are first machined from copper and then given a thin coating of 60 Pb-40 Sn solder. The copper provides the necessary strength, whereas the solder gives a superconducting path and the superconducting contact. Unlike many superconductors, solder is easily applied and repaired by use of simple equipment. Experience has shown that a thin (0.001-in.) layer of solder is more successful than a heavier coating, because a thick application of solder tends to form a ridge where the contacts meet and this ridge causes the switch to open nonuniformly, resulting in a series of voltage pulses to the amplifier rather than one short pulse.

Both single- and double-contact switches have been tried, and at the present stage of design better results have been obtained with double contacts. The center contact is cone-shaped to insure contact with both side plates. The contacts are positioned so that the cone does not wipe across the face of the plates as the switch is opened. Any wiping before the contacts separate produces irregular signals. The two plates must have their contact surfaces in the same plane and be perpendicular to and equidistant from the axis of the center contact.

The contact points are surrounded by a case made of lead which, when superconducting, blocks changes in the magnetic field. This serves to shield the switch from changes in the outside field and also to shield the coil from any fields that may move when the center contact is moved. Switches used for study of lunar samples were shielded by a cylindrical lead case, welded at all joints except one. The welds are difficult to make and also require a higher heat than the rest of the switch would withstand, so the final seam, which must be done with the shield in place, is soldered. The lead welds are used, instead of a solder-lead junction, to reduce thermocouple effects during cooling. By thermocouple effect, induced magnetic fields could be trapped by the shield as it becomes superconducting.

The switch is connected to the detecting coil by three jumbo male banana plugs located at the base of the switch. These plugs are coated with a thin layer of 60 Pb-40 Sn solder, which provides a superconducting contact. The female portions of the banana plugs are mounted in the switch area of the cryostat and are connected to the appropriate circuits. These female portions also have a thin solder coating.

The center contact is attached to a rod made of fiberglass-epoxy laminate which runs to the top of the Dewar. Moving this rod along its axis opens and closes the contacts of the switch. A downward force of 15 to 20 lb is used to hold the contacts closed. If the pressure were applied to the switch mounting platform, movement would occur in many parts of the Dewar, including the detecting coil with respect to the shielding, causing flux variations. Therefore, a stainless steel tube is connected to the switch housing and runs coaxially with the fiberglass-epoxy rod. The closing force is applied downward on the rod but upward on the stainless tube, causing no net force at the mounting plate. Both the fiberglass-epoxy rod and the stainless tube provide relatively low thermal conductivity and a long heat path to the helium-temperature region. Guides between the tube and rod help prevent bowing of the rod as closing pressure is applied.

To prevent air from entering between the rod and the tube, a seal is placed between the two in the region outside the Dewar. In early models, this seal took the form of a small metal bellows. More recent models have used a plastic sleeve made from heat-shrinkable tubing.

By loosening the seal between the rod and the tube, the contacts can be wiped with a rotary motion. This procedure can be used to remove ice or oxides that may form on the contacts, or to find a better alignment position.

A pneumatic cylinder mounted at the top of the stainless tube moves the rod, thus opening and closing the switch contacts. Remote operation is accomplished by using a solenoid valve to pressurize and vent the upper portion of the cylinder while the lower portion is kept at a regulated

pressure. By adjusting pressures, the closing force and opening speed can be controlled. Current capacity is correlated with the pressure between contacts.

There is often some contact wiping during opening. For this reason, opening speed becomes important. Switch-opening speed is most affected by the rate at which gas can be vented from the top of the cylinder. This varies with the type of gas used, volume of hose between cylinder and valve, speed of valve opening, and vent orifice size. In studying Apollo 11 samples, helium gas was used; the solenoid valve had two vent orifices, 1/16 and 3/32 inch in diameter; the cylinder was 0.75 inch in diameter; and 4 ft of 3/8-in.-diameter hose connected the valve and cylinder. Since that time, better results have been obtained by using a valve with a larger vent diameter, attached directly to the cylinder.

A metering valve is placed on the input side of the solenoid valve. This controls the rate of switch closing. It is desirable to take a second or more to close the switch. Closing the contacts quickly soon forms a ridge on the center cone where it meets the contact plates. This ridge causes undesirable wiping as the switch opens. Also, fast closing results in vibrations which reach the detecting coil as the contacts close, causing variations in stored flux. This in turn causes variations in signal size when the switch is opened. In opening, vibrations reach the coil about 9 msec after the contacts have separated, and thus do not affect the measured signal. By closing slowly, the vibrations are reduced in amplitude and damp out before the contacts close, thus storing a nearly uniform flux each time.

If contact travel is kept short, better results are obtained. Downward travel is limited by the contacts of the switch and upward travel is limited by a stop inside the cylinder.

Results

The resistance of this type of switch has been measured and found to be less than $10^{12}\ \Omega$ and consistent with zero as long as the current is less than 20 mA. This permitted testing of samples such as small magnets. In one such test, a magnet with poles of 11500 emu, separated by 2.6 cm, was run in the detector for 1000 passes. The subsequent measurement showed equality between the two poles to better than one part in 3×10^{11}. Although a keeper was on the magnet during this test, currents through the switch were as high as 10 mA while the magnet was inside the coil.

As mentioned in the body of the paper, detector noise for "reference" signals, which require no switch operation, is equivalent to 25 passes of a magnetic charge g_0. The noise of the "short store" and "measurement" signals, which require switch operation, is equivalent to 45 passes of g_0. This gives a value for the switch noise equivalent to about 35 passes of g_0, supposing all the noise increment is due to the switch operation. However, other origins of this increment can be thought of.

Three switches given lifetime tests operated properly after 2500 opening and closing operations, 1400 of which were with a fast closing. One switch began to fail soon afterwards but was easily repaired in 15 minutes by removing the cylinder, seal, and fiberglass-epoxy rod, taking the center contact out of the cryostat, replacing the contact with a newly

tinned part, and reassembling. This was accomplished without warming the major portion of the equipment, and resulted in the loss of about 15 liters of liquid helium when the rod and contact were reinstalled in the cryostat. The banana plugs permit a similar operation to be performed on the whole switch unit, but the design of the top plate of the cryostat prevents their complete removal without a minor disassembly.

If the switches are kept in a helium atmosphere, they can be used after a long period of no operation.

III. Cryogenic Equipment

The cryostat and transport system are represented in Fig. 4.

The sensing coil is one of the primary elements of the detector. The coil, 5.25 in. inside diameter by 10 in. long, has 1308 turns of fully annealed 0.020-in.-diameter niobium wire insulated with Formvar. For operational reliability three separate circuits, each consisting of a coil and a switch, were installed. The three coils were wound tri-filar. In our mode, two switches must be open when the third one is active.

To minimize any loss or transfer of flux energy when the switch is opened, all closed metallic loops are located a minimum distance of one diameter (5 in.) from the sensing coil. This dictates plastic walls in the sensing area. The inner tube of the liquid helium vessel is 5-in. i.d. × 1/8-in. wall × 59-in. long, filament-wound fiberglass-epoxy. The ambient inner wall of the vacuum vessel is 3.58 in. o.d. × 0.110 in. wall × 65 in. long, filament-wound fiberglass-epoxy. Both tube ends are epoxy bonded to 0.020-in. stainless steel diaphragm sections which are later permanently welded into the vessels and connections. These thin diaphragms allow transition-joint techniques at assembly and also

compensate for thermal stress during temperature excursions. In addition, the ambient tube diaphragms, with a few extra convolutions, provide noise isolation of the transit system from the cryostat.

Preliminary tests on a short tube section (Fig. 11), 5 in. in diam 12 in. long, showed that although the fiberglass-epoxy didn't have a vacuum leak it did have a diffusion rate. This helium permeation rate seemed to increase with decreasing temperature;[12] there is no apparent permeation at 293°K, but at 4.2°K it is 0.7 to 2.8×10^{-11} cc/sec/in.^{2}. Thus for a LHe system, a dynamic or continuously pumped insulating vacuum system was needed. The fiberglass-epoxy tube test section was cycled and shocked many times from room temperature to 77°K and 4°K.

Thermal radiation shielding for the 5-ft-long ambient hole is provided by about 0.500 in. (~ 130 turns) of aluminum-coated 0.00025-in. Mylar. The Mylar is coated on one side only, and is wound nonconductively as a continuous nonconnected spiral. To speed vacuum pumpdown 0.75-in. holes are punched on 6-in. centers. Heat leak for this ≈ 7 ft^2 of 4°K area is estimated at 1 to 1.3 watt. Temperature measured during operation at the midpoint of the bore tube was only 1°C below ambient. All other areas of the LHe vessel are thermally shielded by shields cooled by liquid-nitrogen (LN).

If the external magnetic field changes or if the coil moves in an ambient field spurious signals are introduced. A lead shield (99.90% Pb) is formed around both ends of the bore tube and 5 in. distant from the sensing coil. If the shield length is 4 times the hole diameter, external field variation effects are reduced by 10^6. These requirements fix the

dimensions of the LHe vessel at 15 in. diam in the center and 60 in. long. To reduce any trapped currents and fields in the lead due to thermocouple effects during cooldown, the lead is electrically insulated from the stainless steel LHe vessel with 0.003-in. Mylar.

The necessity of isolating the lead from the LHe vessel required that an independent lead vessel be built. A fiberglass-epoxy (Nema G-10) ribbed structure supports the lead and provides a construction framework. Figure 12 shows the ribbed structure, together with the sensing coil in place and the LHe fill-and-empty tube extending to the bottom of the LHe vessel. Figure 13, a closeup, shows the wire bundle leaving the coil, and Fig. 14 shows the lead in place on each end. The lower LN shield is visible in the left background. To further minimize thermocouple effects in the lead, the joints and seams were joined by lead welding; no alloying elements were used.

After the structure in Fig. 14 is covered with the 0.060-in. sheet lead, it is wrapped with 0.003-in. Mylar. Then it is inserted into the stainless steel vessel shown in Fig. 15 and the circumferential seams are heliarc welded. The need to isolate the lead from the LHe vessel, as well as the need for reliable vacuum joints, requires careful and logical sequential assembly techniques.

A 45-liter LHe reservoir is located above the coils. The switch plate is mounted at the base of this reservoir and outside the primary lead shield. The top of the reservoir is closed with a 15-in. diam flange, 0.5-in.-diam bolts 2 in. on center, and a 0.060-in.-diam indium gasket crushed to ≈ 0.005 in.

The cryostat, following good cryogenic (as well as magnetic) practice, is constructed of nonmagnetic, nonferritic material. The vacuum tank is aluminum, the LN shields are copper, and the LHe vessel is austenitic stainless steel. The vacuum tank, together with the transit system partially assembled, is seen in Fig. 16. For vibration isolation in operation, the vacuum tank is mounted on Isomode rubber pads, the transit system is separate from the cryostat, and all vacuum and cryogenic lines to the cryostat are flexible hose.

The insulating vacuum system consists of a 4-in. water-cooled oil diffusion pump, with a speed of 750 liters/sec and an ultimate pressure of 10^{-9} Torr. A two-stage mechanical pump of 17.7 cfm capacity provides the forevacuum. Pressure is monitored with thermocouple and ion gages. Pressure rise, power failure, and overtemperature are interlocked with a 6-in. diam air-operated valve on the forevacuum line to provide vacuum system isolation. Emergency pressure relief for the vacuum tank is provided by backing off all the bolts 3/8 in. on the main tank flange.

Cryostat Operations

The equipment has had two test operations in Berkeley and four operations in Houston, including the Apollo 11 mission in August 1969. Length of operation in each case was about 5 to 7 days. Temperature transients were handled carefully, cooldown to 77°K was at the maximum rate of 50°C per hour. Warmups from 4°K took 12 to 15 hours by heat transfer to atmosphere via 300 to 500 μ of He gas in the insulating vacuum space.

To minimize effects of earth field trapped by the lead, a system of coils outside the cryostat reduces the field in the sensing region to a few milligauss while the assembly is cooled to LHe and the lead goes superconducting. After LHe cooldown the sensing circuits are tested for superconductivity by time measurements of current storage.

Operations behind the biological barrier of the Lunar Receiving Laboratory required limited access and exit. There was no opportunity to remove supply Dewars, therefore all LHe was carefully rationed and closely monitored. LHe was supplied in 500-liter Dewars, weighed initially and continuously during use with a strain-gage load cell system. Also, the LHe transfer line had an in-line sight gage. Both devices allowed continuous monitoring and determination of transfer valve leakage, and helped to hold transfer losses to a minimum.

Cryostat LHe loss, as measured on a fixed-increment carbon resistor stick, was 6 liters per hour ≈ 4.2 watts. For a 5-ft-long ambient hole, this is less than the first approximation value of 1 watt per foot of cryostat length. The ambient hole loss is estimated at about 1 watt, major losses being conduction down the neck, switch actuators, and wires.

IV. Monopole Lunar Sample Container

For diagram and photographs of the container see Figs. 7, 17, and 18.

Two seal requirements were specified by the Lunar Receiving Laboratory, NASA-MSC, Houston. They were:

1. A seal leak rate of less than 10^{-7} std cm^3/sec of helium.

c. A drop test from a 4-foot height which the container must withstand without exceeding the above leak rate.

In addition, careful material control was necessary, as hydrocarbons and radioactive elements were undesirable. Indium seals were preferred over elastomers.

It is hard, easy to obtain vacuumtight seals with indium, even with imperfect surfaces, if one has large clamping forces available. The container was designed to pass the maximum amount of lunar material through the cryostat access hole of 3.375 in. i.d. It is modeled somewhat after the astronaut contingency container -the ALSRC (Apollo lunar sample return container)- that was loaded immediately on the lunar surface and placed in a pocket of the astronaut suit. Maximizing the can size and minimizing the weight eliminates large heavy flanges and many circumferential bolts.

Also, the added constraint of operation with astronaut gloves in the vacuum complex requires a simple, easy assembly. Therefore the lid is designed as a one piece assembly with preplaced indium. A single clamp does not provide large forces. Therefore the seal surfaces must be kept reasonably undamaged before a seal is attempted. The indium surface may have minor scratches; indium flows easily and welds to itself. The stainless steel polished edge (0.030 in. wide to increase the unit loading) cannot have any radial scratches, nicks, or dents. The parts are made of austenitic stainless steel and the container holds about 250 milliliters.

The first seals were made by electroplating 0.006 in. of indium on the lid surface. The latest process is to ultrasonically tin the stainless

steel surface with indium, press a 0.060-in.-diam wire (99.999% In) to 0.015 in. thickness, and trim the flash. As indium welds to itself, this produces a solid, well-bonded surface capable of surviving the required aerospace cleaning techniques (contaminant level less than 1 mg/cm^2).

In use, the indium lid surface is clamped against the 0.050-in.-wide land on the can body with a triangular spring plate and a 1/2"-20 UNF bolt. The bolt is electroplated with 0.0003 in. of silver to prevent galling, and the spring plate compensates for thermal changes and indium creep.

The container satisfied the vacuum-seal, drop-test, and material requirements of NASA.[13]

Successful indium seals (leak rate $< 10^{-9}$ std cm^3/sec) and reseals up to 10 times are achieved with torques of 25 in.-lb, although a minimum of 50 in.-lb is recommended for application.

V. Circuit Diagrams

Circuit diagrams are shown in Figs. 19 and 20. The values for the resistances and capacitors in Fig. 20 are given below.

R_1 = 1.6	MΩ	r_1 = 16	kΩ	ρ_1 = 160	kΩ
R_2 = 820	kΩ	r_2 = 8.2	kΩ	ρ_2 = 82	kΩ
R_3 = 43	kΩ	r_3 = 4.3	kΩ	ρ_3 = 43	kΩ
R_4 = 22	kΩ	r_4 = 2.2	kΩ	ρ_4 = 22	kΩ
R_5 = 100	kΩ	r_5 = 1.0	kΩ	ρ_5 = 10	kΩ
		r_6 = 1.0	kΩ		
C_1 = 4700	pF	C_1 = 47	pF	Y_1 = 470	pF
C_2 = 0.01	μF	C_2 = 100	pF	Y_2 = 1000	pF
C_3 = 0.022	μF	C_3 = 220	pF	Y_3 = 2200	pF
C_4 = 0.047	μF	C_4 = 400	pF	Y_4 = 4000	pF
C_5 = 10	μF	C_5 = 0.1	μF	Y_5 = 1	μF
		C_6 = 0.33	μF		

FOOTNOTES AND REFERENCES

*Work done under auspices of the U. S. Atomic Energy Commission and the National Aeronautics and Space Administration.

†Stanford Linear Accelerator Center, Stanford, California.

1. P. A. M. Dirac, Quantized Singularities in the Electromagnetic Field, Proc. Roy. Soc. London A133, 60 (1931); P. Dirac, Phys. Rev. 74, 817 (1948).

2. (a) J. Prescott, E. H. Carlson, V. W. Hughes, Bull. Amer. Phys. Soc. 13, 630 (1968) (paper E 17); J. G. King, Phys. Rev. Lett. 5, 562 (1960).

3. L. Schiff, Phys. Rev. 144, 1087 (1966); Science 165, 757 (1969).

4. (a) I. Zhuravlev, E. Kh. Khakimov, V. P. Martemianov, S. P. Denisov, V. V. Demtsov, V. G. Tarasenkov, Phys. Letters 31B, 477 (1970).

(b) For a systematic review of experimental searches for Dirac monopoles up to 1968, we refer the reader to F. Arnaldi, On the Dirac Magnetic Poles, in Old and New Problems in Elementary Particles, Ed. by G. Puppi (Academic Press, New York, 1968), page 30. Three more recent searches are reported in Refs. 4 and 6.

(c) R. L. Fleischer, H. R. Hart, I. S. Jacobs, P. B. Price, W. M. Schwarz, and F. Aumento, Phys. Rev. 184, 1393 (1969) and R. L. Fleischer, P. B. Price, and R. T. Woods, Phys. Rev. 184, 1398 (1969).

5. L. W. Alvarez, Proposal to NASA to Search for Magnetic Monopoles in Returned Samples of Moon Surface Material, Jan. 30, 1966.

6. The Lunar Receiving Laboratory, located at the Manned Spacecraft

Center in Houston, Texas, is where lunar samples were returned and had to be studied prior to their distribution throughout the world.

9. L. W. Alvarez, Physics Note No. 470 (1963), unpublished.

10. P. Eberhard, Physics Note No. 506 (1964), unpublished.

11. L. Alvarez, P. Eberhard, R. Ross and R. Watt, Science 167, 701 (1970).

12. J. Harvey, LRL Engineering Note M4236.

13. E. Hoyer, LRL Engineering Note M4162C.

Table I. Changes equivalent to one pass of a magnetic charge g_0 through the detector.

1. Flux per turn of the coil = Φ_0 =	4.04×10^{-7} G-cm^2
2. Flux detected in the sensing coil corrected for reduction effect of shield =	4.1×10^{-4} G-cm^2
3. Current in sensing coil =	54 pA
4. Current in auxiliary coil =	19.5 nA
5. Magnetic field along the axis and in the center of sensing coil =	2.4 nG
6. Magnetic dipole along the axis and in the center of sensing coil	9.1×10^{-7} emu
7. $\frac{1}{2}\frac{(\Delta I)^2}{}$	7×10^{-4} eV

FIGURE CAPTIONS

Fig. 1. Superconducting loop used for detection.

Fig. 2. Sketch of monopole detector and electronic circuits.

Fig. 3. Superconducting switch.

Fig. 4. Cryostat and transport system.

Fig. 5. Signal display: 1 is the reference signal, 2 the short-store signal, 3 the measurement signal. V is the amplitude of the measurement signal.

Fig. 6. Sketch of amplifier circuit. The circuits R1 C1, R2 C2, and R3 C3 have the same time constant.

Fig. 7. Sample container.

Fig. 8. Equipment installed in the Lunar Receiving Laboratory.

Fig. 9. Electric field surrounding the path of a moving monopole.

Fig. 10. Parts of the superconducting switch.

Fig. 11. Fiberglass tube test section.

Fig. 12. Rib structure, fill tube, and sensing coil.

Fig. 13. Wires to sensing coil.

Fig. 14. Rib structure prior to lead wrapping.

Fig. 15. Parts of liquid helium vessel.

Fig. 16. Vacuum tank and transit system.

Fig. 17. Sample container parts.

Fig. 18. Sample container, assembled.

Fig. 19. Electronic block diagram.

Fig. 20. Amplifier

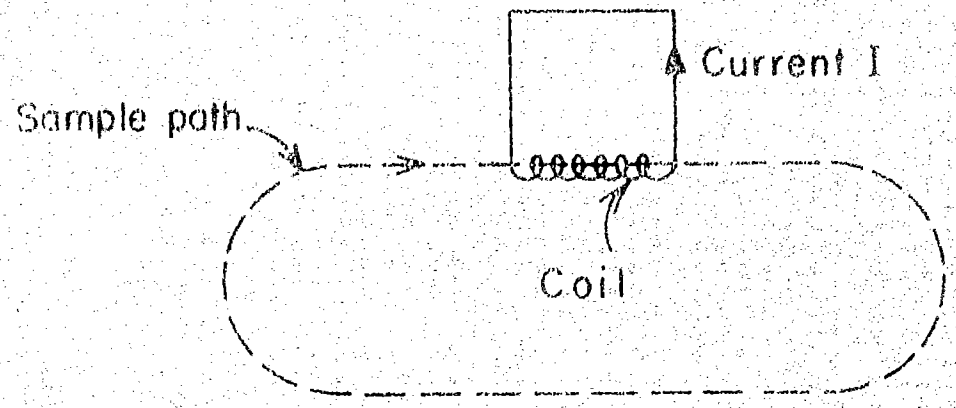

Fig. 4

XBL704-2698

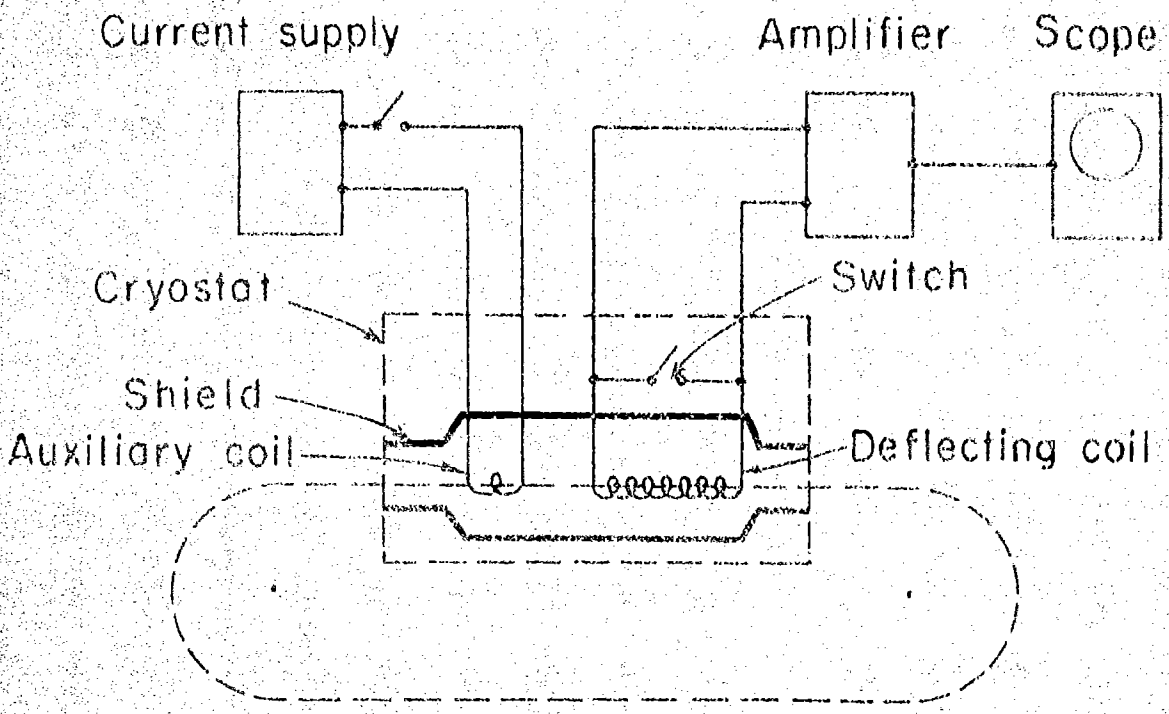

Fig. 2

XBL704-2699

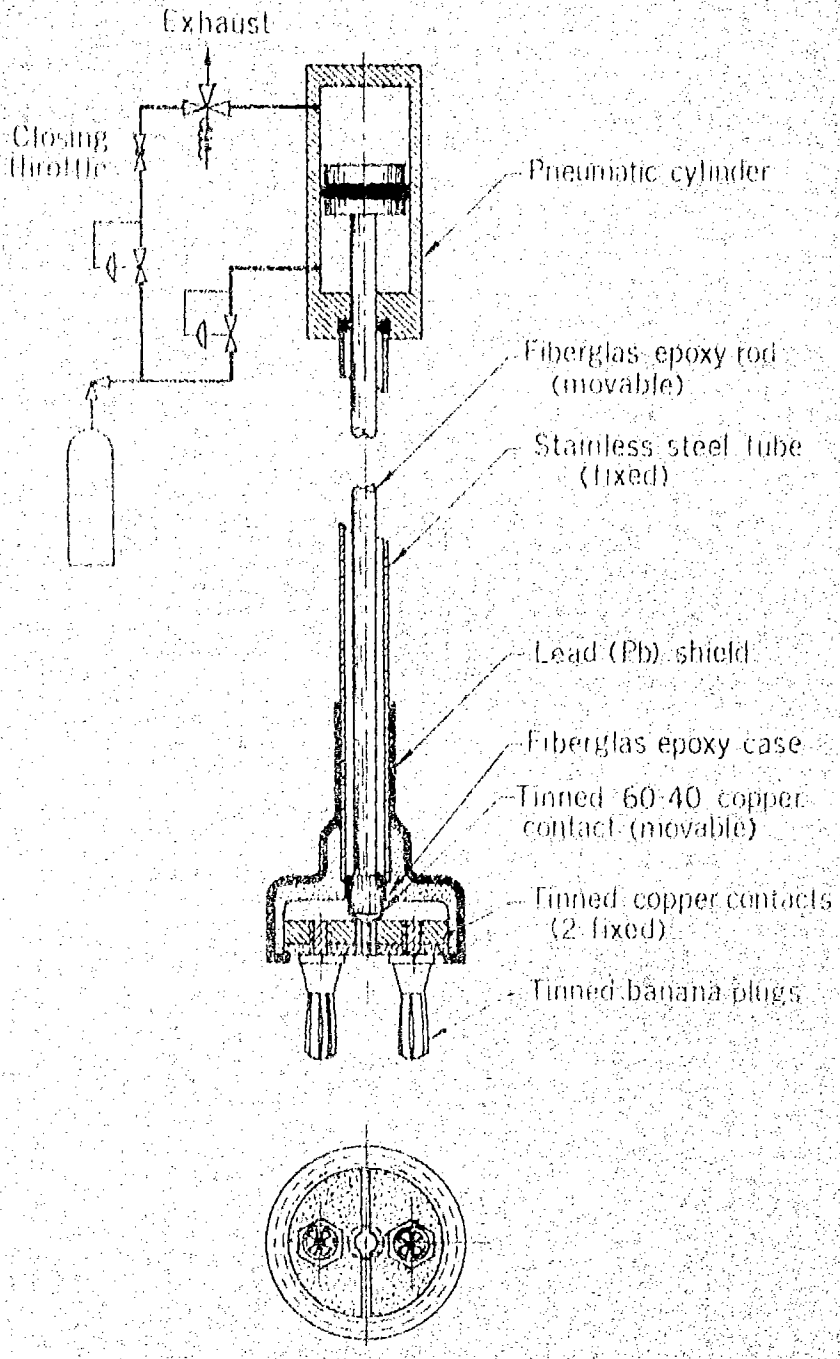

Fig. 3

XBL 702-6138

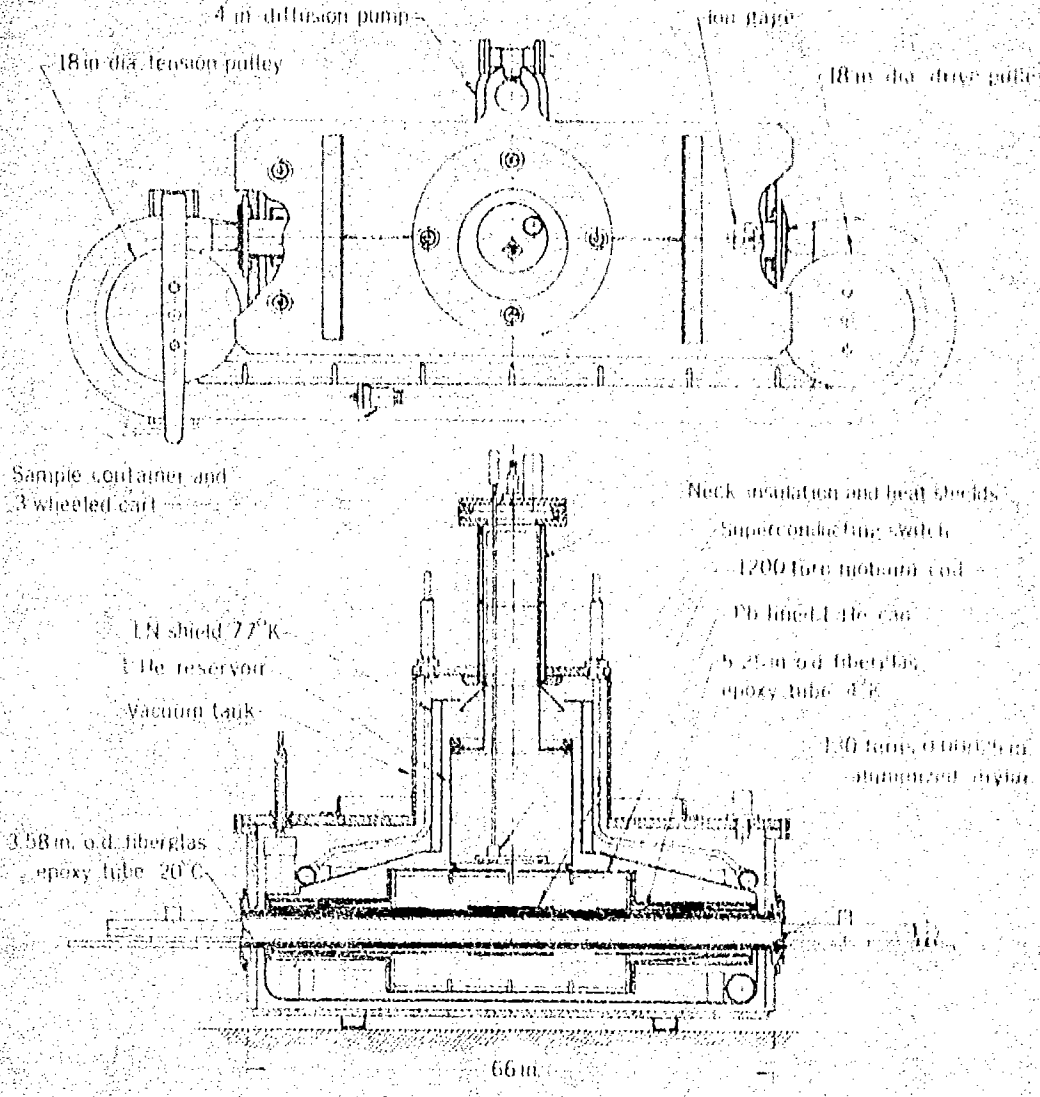
4 in. diffusion pump
ion gage
18 in. dia. tension pulley
18 in. dia. drive pulley
Sample container and
3 wheeled cart
Neck insulation and heat shields
Superconducting switch
1200 turn niobium coil
Pb lined LHe can
LN shield 77°K
LHe reservoir
Vacuum tank
3.58 in. o.d. fiberglas
epoxy tube 20°C
66 in.

Fig. 4

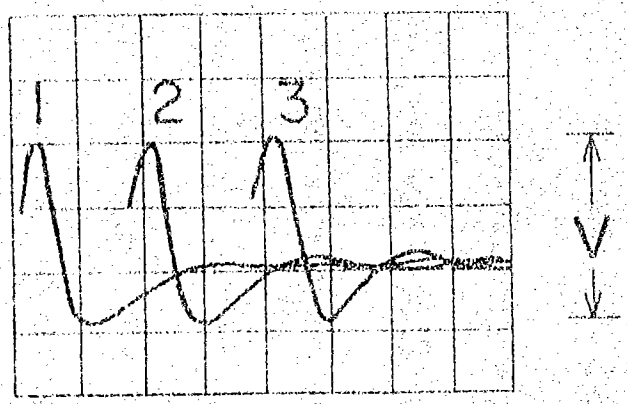

Fig. 5

XBL704-2696

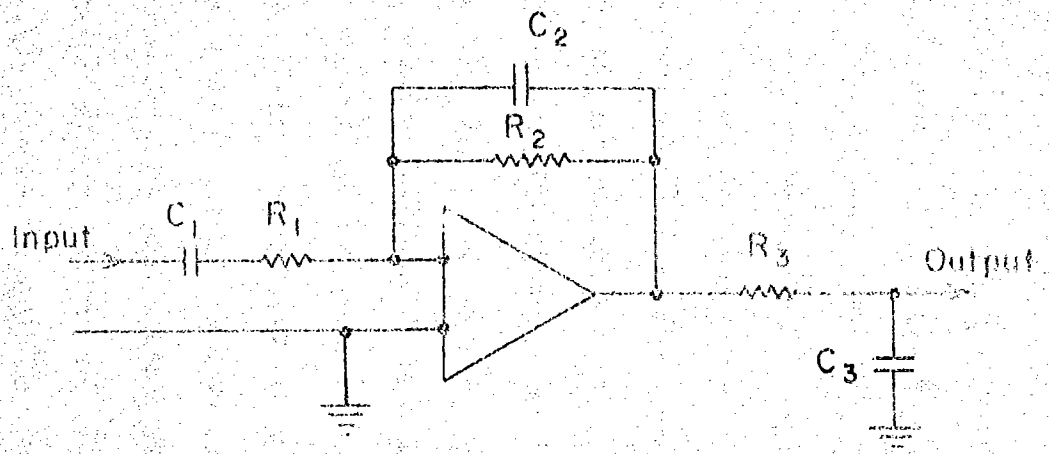

Fig. 6

XBL704-2697

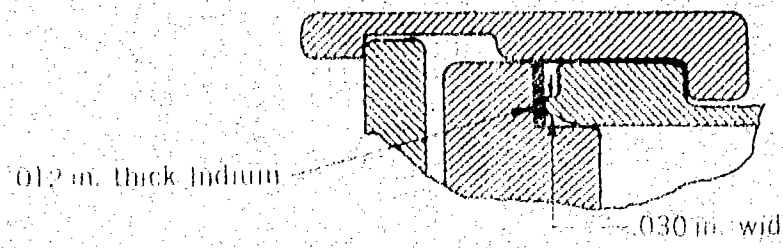

Seal detail

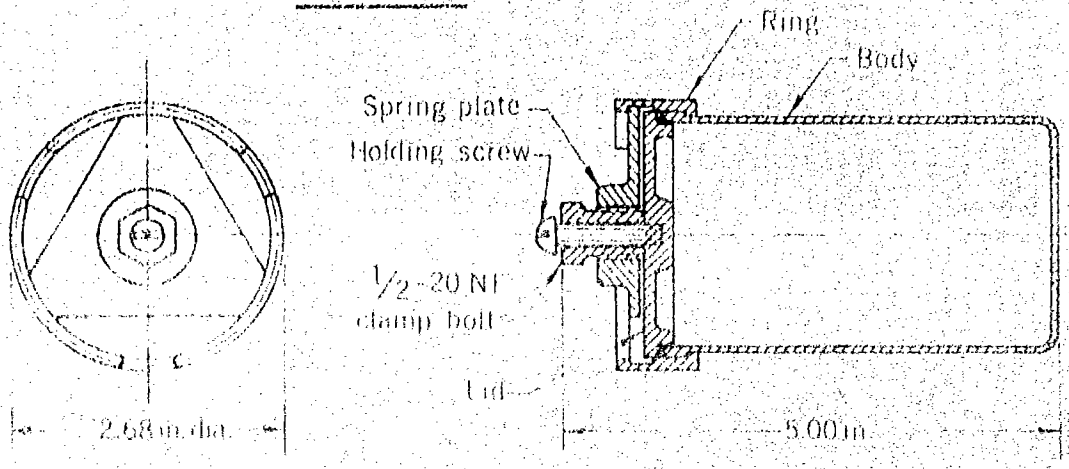

Fig. 7

XBL 702 6137

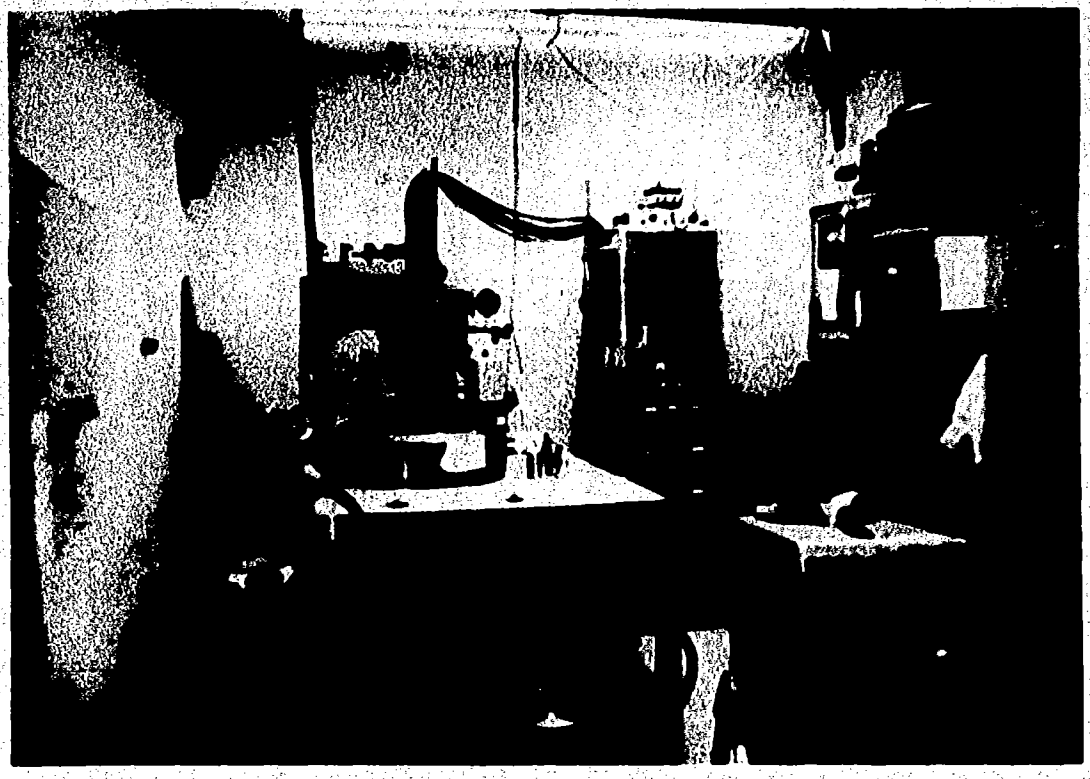

Fig. 8 CBB702-963

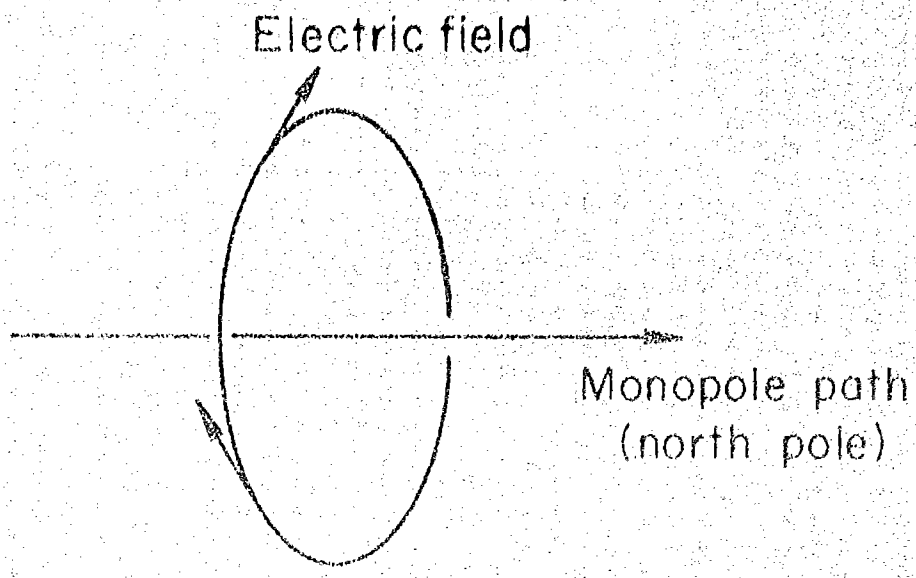

Fig. 9

XBL6912-6392

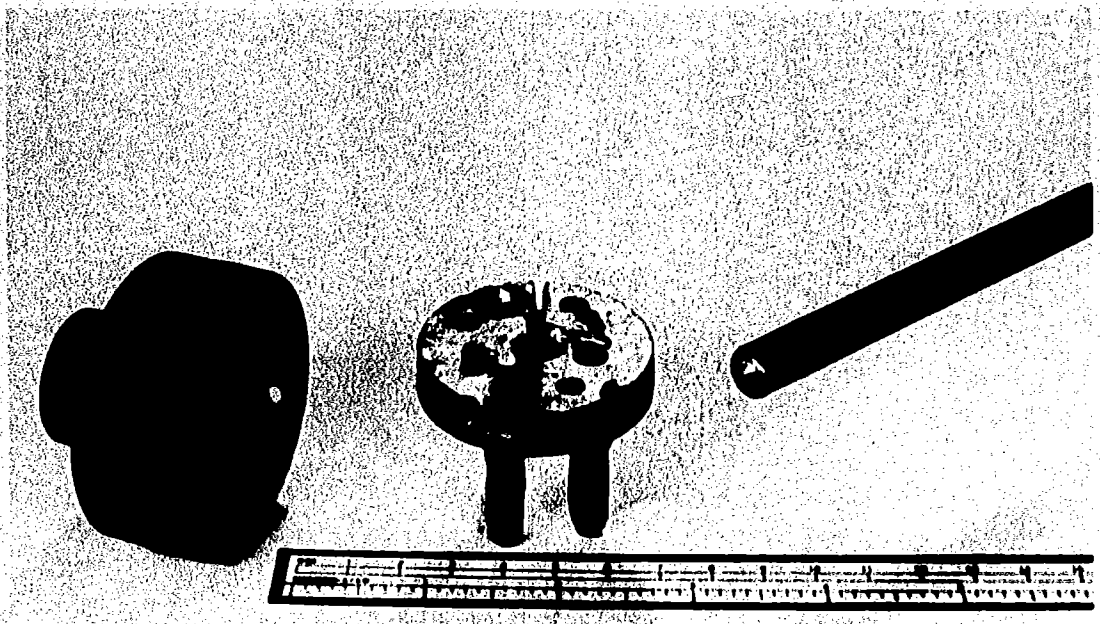

Fig. 10

CBB702-1100

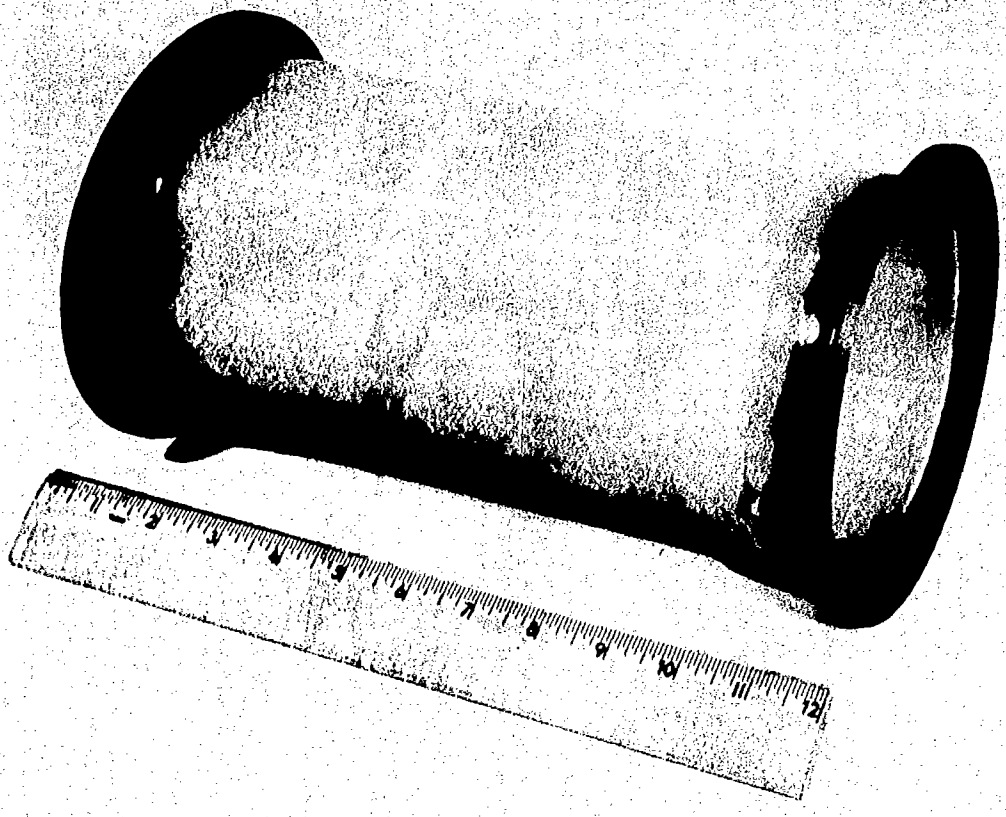

Fig. 11

XBB683-1384

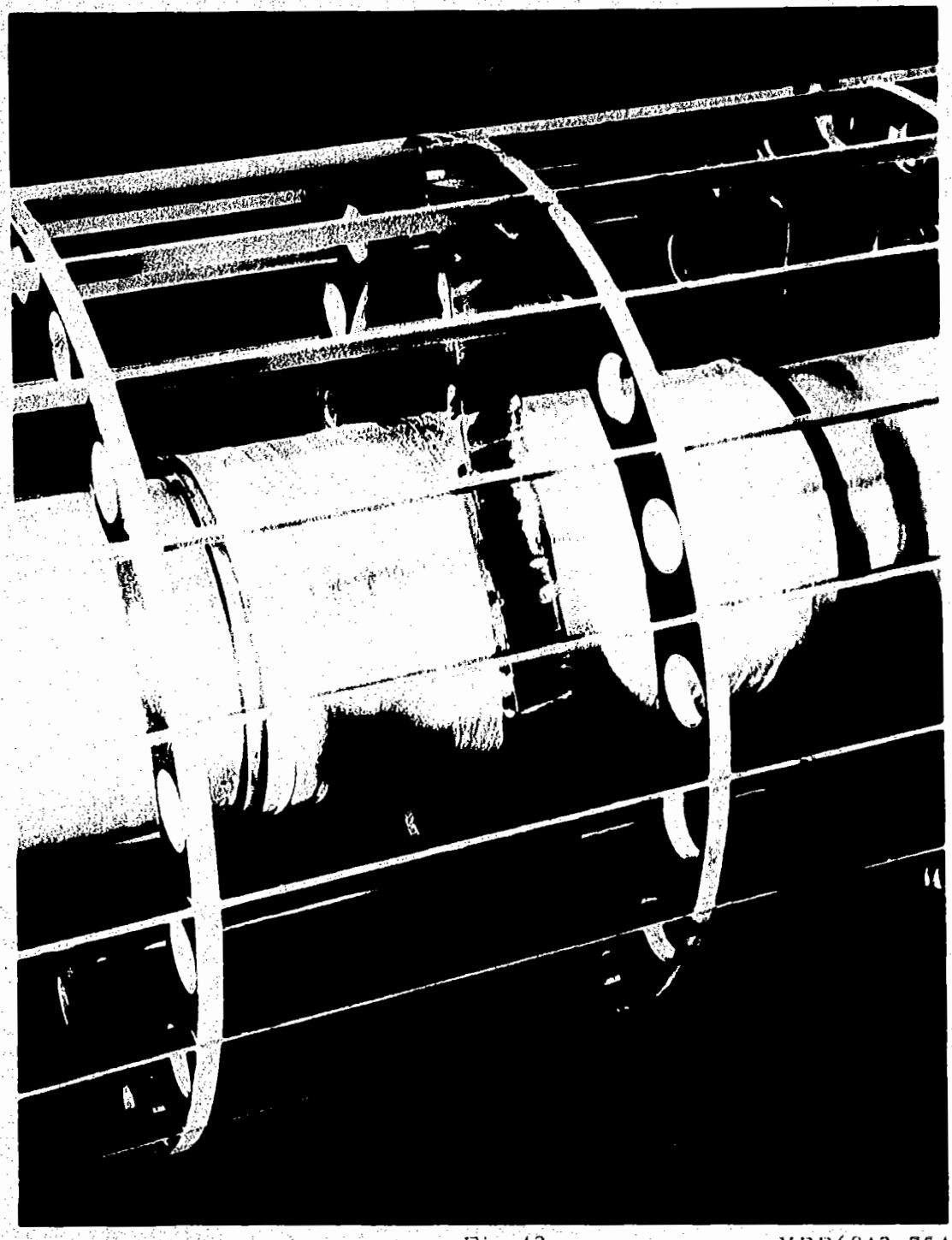

Fig. 12

XBB6812-7549

Fig. 13 XBB6812-7548

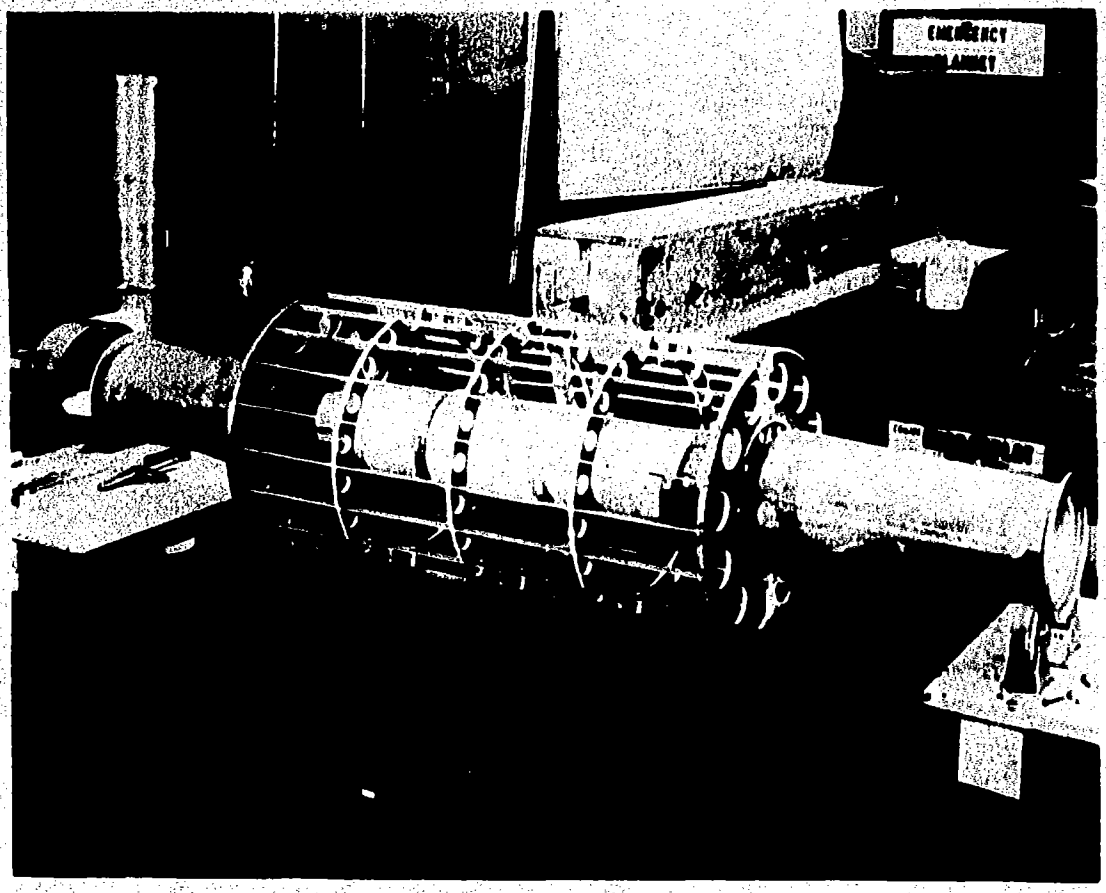

Fig. 14

XBB6812-7547

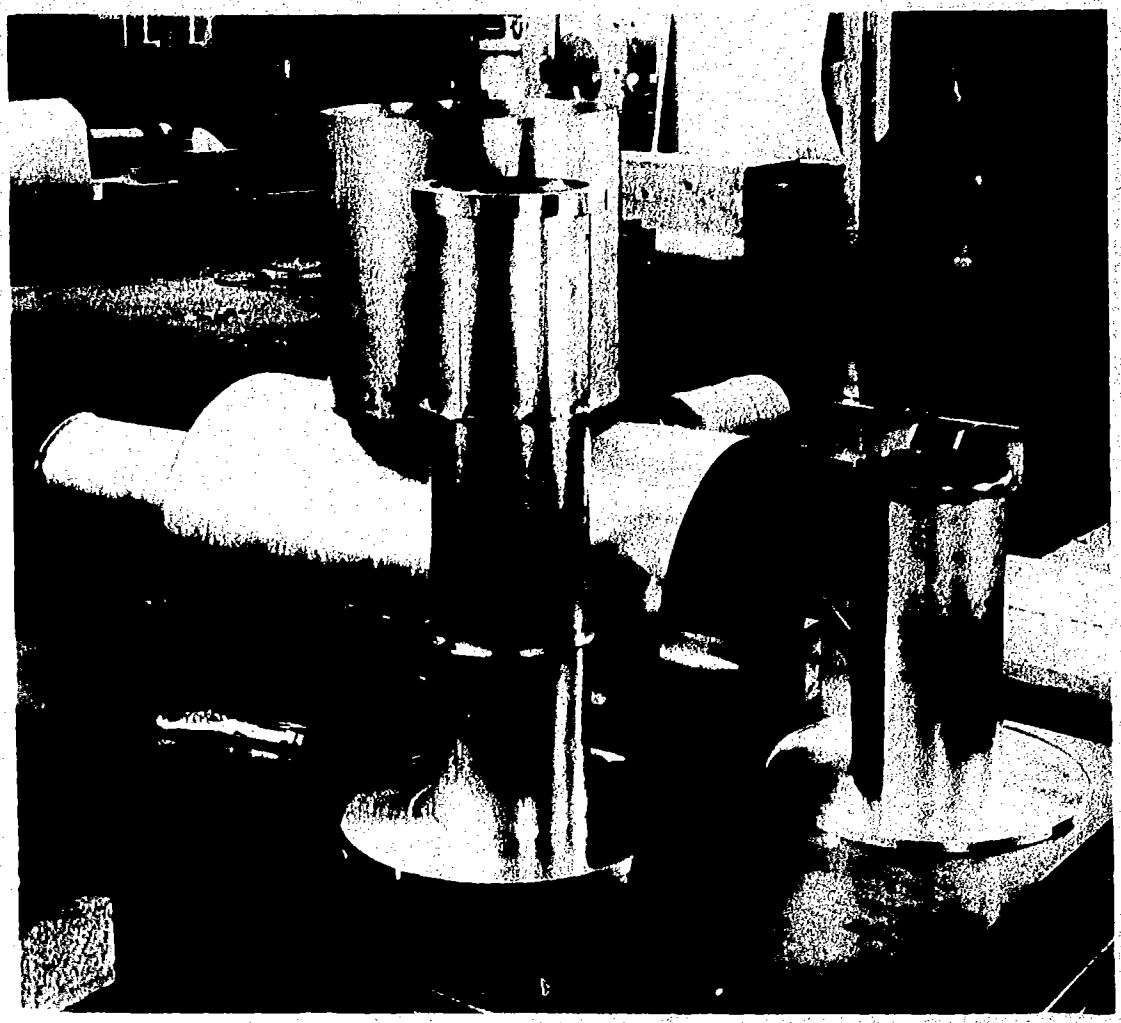

Fig. 15 XBB6812-7552

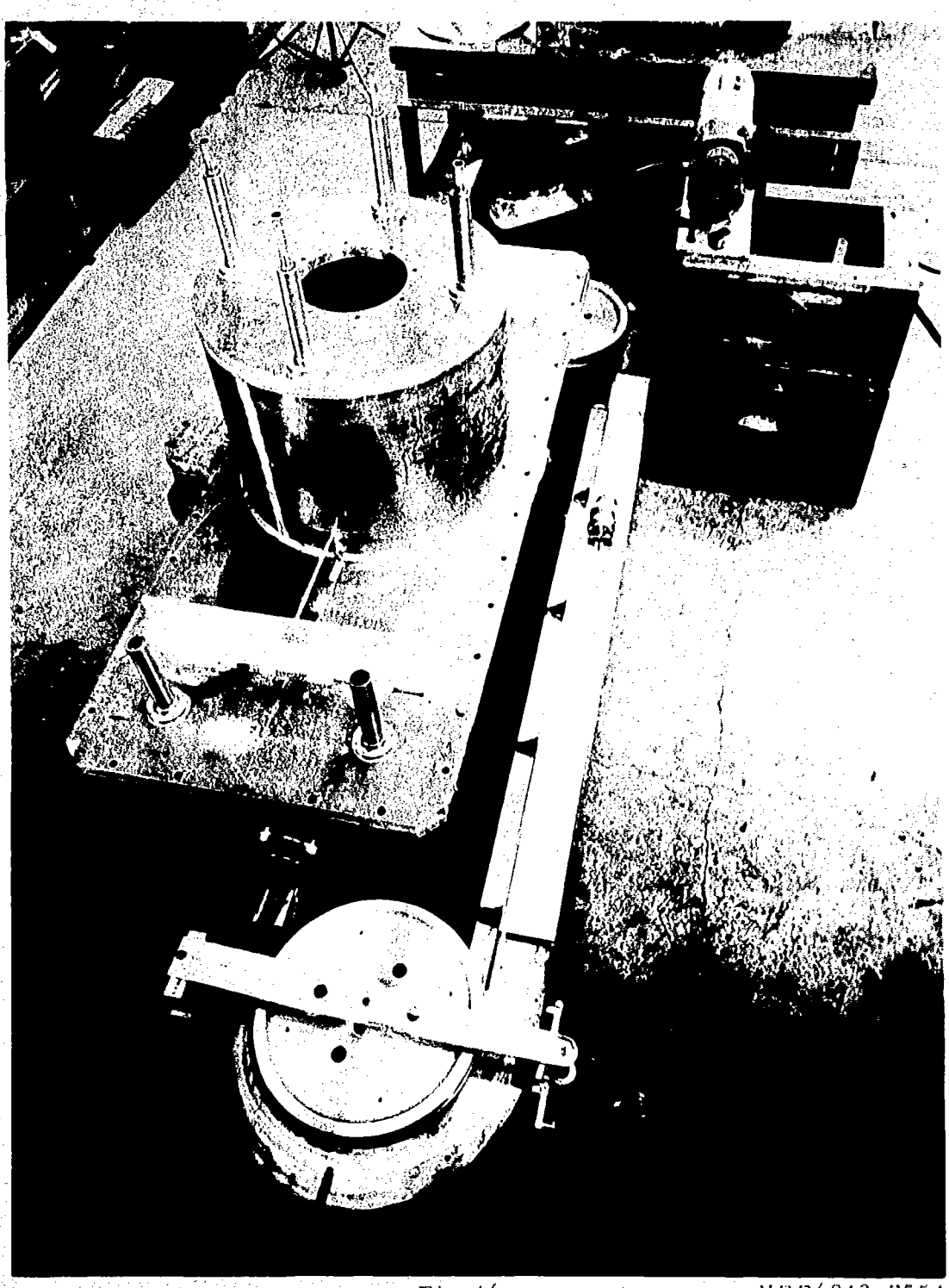

Fig. 16 XBB6812-7554

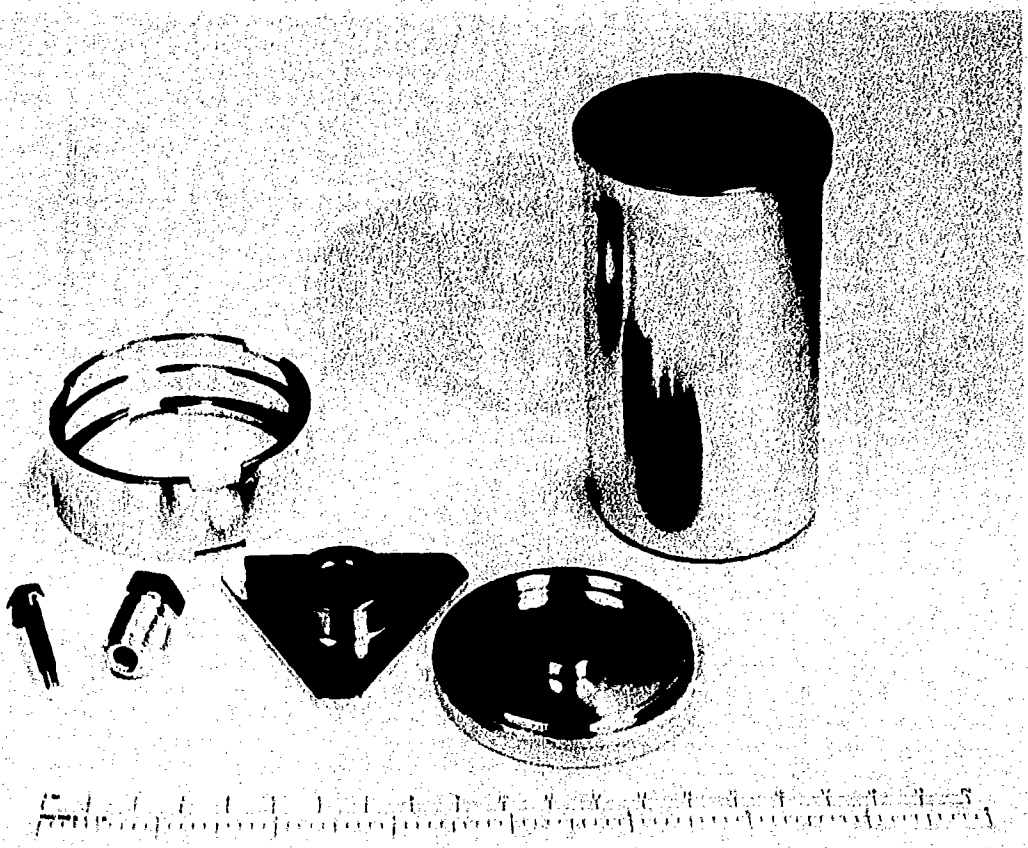

Fig. 17

XBB694-2490

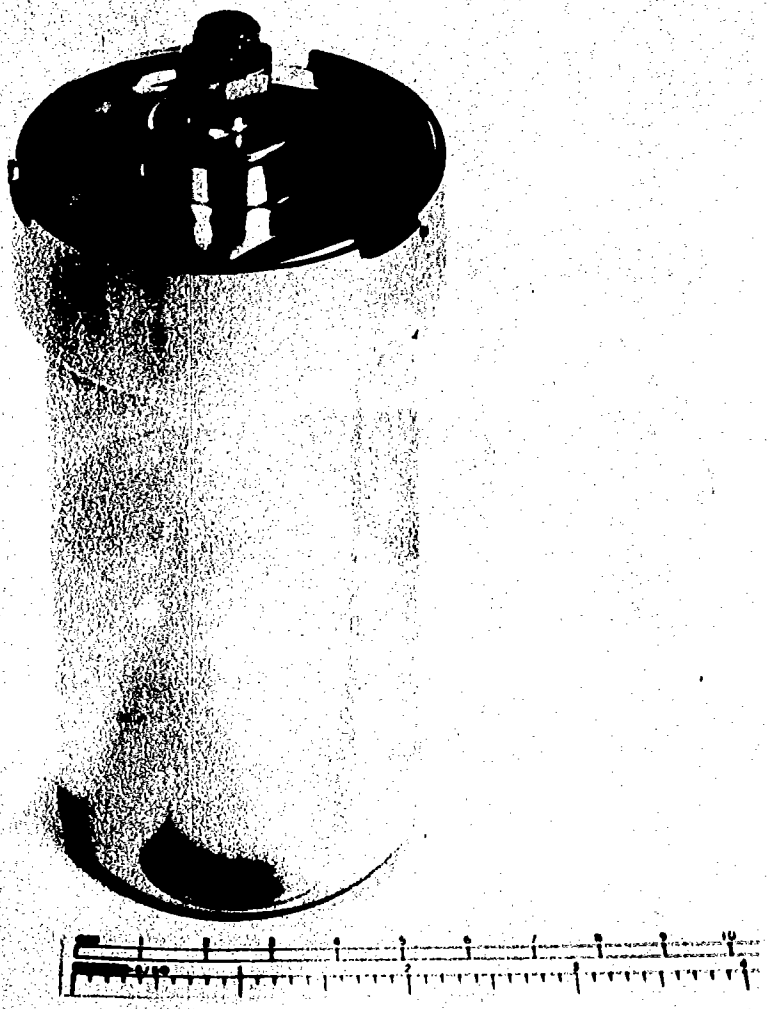

Fig. 18 XBB694-2491

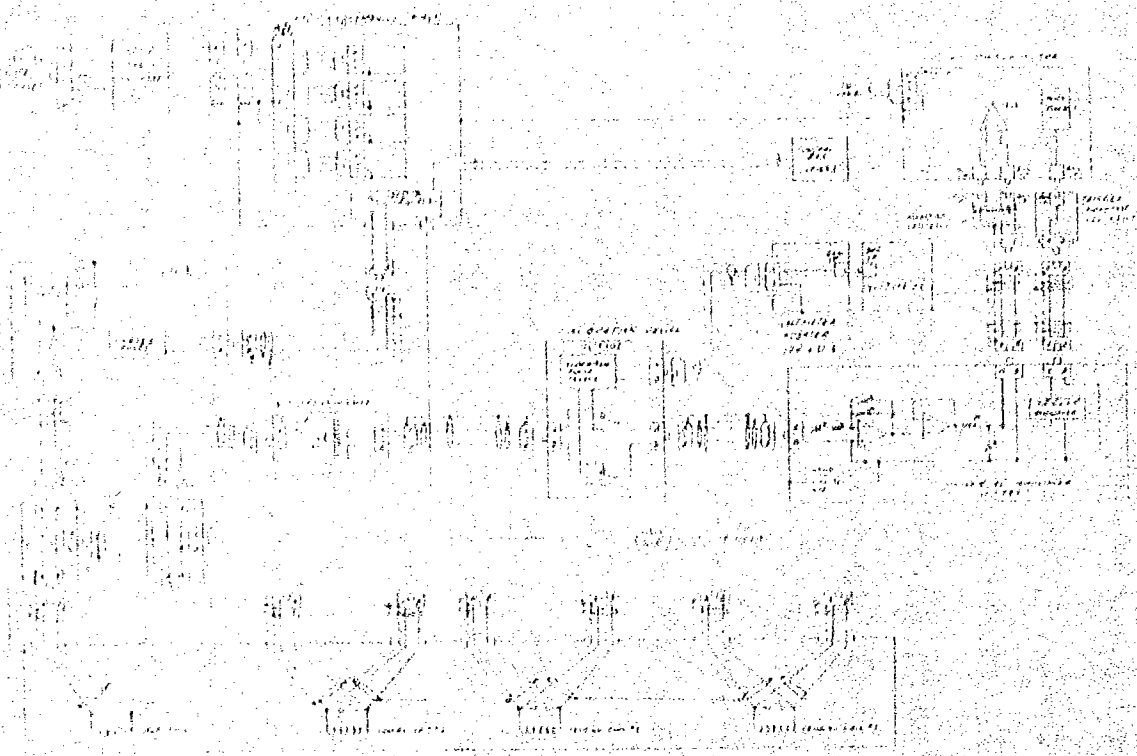

XBL 704-851

Fig. 19